### Please cite the Published Version

Jantalika, Tanachapa, Manochantr, Sirikul, Kheolamai, Pakpoom, Tantikanlayaporn, Duangrat, Pinlaor, Somchai, Saijuntha, Weerachai, Paraoan, Luminita and Tantrawatpan, Chairat (2025) Human chorion and placental mesenchymal stem cells conditioned media suppress cell migration and invasion by inhibiting the PI3K/AKT pathway in cholangiocarcinoma. Scientific Reports, 15. 31472 ISSN 2045-2322

**DOI:** https://doi.org/10.1038/s41598-025-16789-6

**Publisher:** Springer Nature **Version:** Published Version

Downloaded from: https://e-space.mmu.ac.uk/641563/

Usage rights: Creative Commons: Attribution-Noncommercial-No Deriva-

tive Works 4.0

**Additional Information:** This is an open access article published in Scientific Reports, by Springer Nature.

**Data Access Statement:** All data generated or analysed during this study are included in this published article and its supplementary information files.

### **Enquiries:**

If you have questions about this document, contact openresearch@mmu.ac.uk. Please include the URL of the record in e-space. If you believe that your, or a third party's rights have been compromised through this document please see our Take Down policy (available from https://www.mmu.ac.uk/library/using-the-library/policies-and-guidelines)

# scientific reports



## **OPEN**

# Human chorion and placental mesenchymal stem cells conditioned media suppress cell migration and invasion by inhibiting the PI3K/AKT pathway in cholangiocarcinoma

Tanachapa Jantalika<sup>1,2</sup>, Sirikul Manochantr<sup>1,2</sup>, Pakpoom Kheolamai<sup>1,2</sup>, Duangrat Tantikanlayaporn<sup>1,2</sup>, Somchai Pinlaor<sup>3</sup>, Weerachai Saijuntha<sup>4</sup>, Luminita Paraoan<sup>5⊠</sup> & Chairat Tantrawatpan<sup>1,2⊠</sup>

Cholangiocarcinoma (CCA) is an aggressive bile duct malignancy with poor survival rates due to late detection, rapid metastasis, and treatment resistance. Therefore, new therapeutic strategies are needed to improve treatment outcomes. Previous studies have reported that mesenchymal stem cells (MSCs) secrete several soluble factors that modulate intracellular signaling pathways that are critical for the regulation of cancer cell function. The present study aimed to investigate the effects and molecular mechanisms of conditioned media from chorion-derived human MSCs (CH-CM) and placenta-derived human MSCs (PL-CM) on the migration and invasion of human CCA cells. We found that both CH-CM and PL-CM suppress cell migration and invasion in three CCA cell lines (KKU100, KKU213A and KKU213B) by increasing E-cadherin expression and decreasing the expression of several factors involved in the epithelial–mesenchymal transition process, including ZEB1, ZEB2, N-cadherin, vimentin, and MMP-2. The effects of CH-CM and PL-CM were mediated, at least in part, through the suppression of the PI3K/AKT signaling pathway in CCA cells. Our findings suggest that soluble factors derived from CH-MSCs and PL-MSCs could be used in combination with other conventional treatments to diminish the invasiveness of CCA cells, thus improving the therapeutic outcome and increasing survival in CCA patients.

**Keywords** Mesenchymal stem cells, Bile duct cancer, Migration, Invasion, PI3K/AKT pathway

Cholangiocarcinoma (CCA) is an aggressive malignancy that develops from damaged epithelial cells in various parts of the biliary tract, including the intrahepatic and extrahepatic bile ducts<sup>1</sup>. Advanced-stage CCA is prevalent in many countries around the world<sup>2</sup> and has a very high mortality rate<sup>3,4</sup> because of its delayed diagnosis, rapid metastasis, and resistance to treatment<sup>5</sup>. Currently, surgical resection is the only therapeutic option for curing CCA, but it is applicable only to a minority of patients, whereas 70–80% of patients who have distant metastasis or locally unresectable tumors rely on mostly ineffective chemotherapy<sup>6,7</sup>. Therefore, new therapeutic strategies are needed to better control tumors and improve the treatment outcome of patients with advanced-stage CCA.

Previous research has shown that the PI3K/AKT signaling pathway plays a critical role in the development and progression of CCA by increasing the proliferation, migration and invasion of CCA cells<sup>8,9</sup>. PI3K is a lipid kinase that generates phosphatidylinositol-(3,4,5)-P3 (PIP3), which phosphorylates and activates Akt, a serine/

<sup>1</sup>Division of Cell Biology, Department of Preclinical Sciences, Faculty of Medicine, Thammasat University, Pathum Thani 12120, Thailand. <sup>2</sup>Center of Excellence in Stem Cell Research and Innovation, Thammasat University, Pathum Thani 12120, Thailand. <sup>3</sup>Department of Parasitology, Faculty of Medicine, Khon Kaen University, Khon Kaen 40002, Thailand. <sup>4</sup>Faculty of Medicine, Mahasarakham University, Maha Sarakham 44000, Thailand. <sup>5</sup>Department of Life Sciences, Manchester Metropolitan University, John Dalton Building, Chester Street, Manchester M1 5GD, UK. <sup>™</sup>email: L.Paraoan@mmu.ac.uk; tchairat@tu.ac.th

threonine kinase, which in turn regulates many genes involved in the progression and metastasis of several cancers<sup>10</sup>, including CCA<sup>11</sup>. As a result, the PI3K/AKT pathway is one of the key targets for the development of new CCA treatments.

Human mesenchymal stem cells (MSCs) are multipotent adult stem cells that have the ability to self-renew and differentiate into several cell types, including adipocytes, chondrocytes and osteocytes<sup>12</sup>. Furthermore, MSCs also release many clinically beneficial soluble factors that affect the growth and metastasis of cancer cells by modulating various signaling pathways<sup>13</sup>, including PI3K/AKT signaling in various cancer cell types<sup>14</sup>, including non-small cell lung cancer<sup>15</sup>, colorectal cancer<sup>16</sup> and breast cancer<sup>17</sup>.

MSCs can be isolated from various adult tissues, such as bone marrow, adipose tissue, and gestational tissue<sup>18</sup>. Compared with other sources of MSCs, chorion- and placenta-derived MSCs (CH-MSCs and PL-MSCs) are the most abundant, easy to obtain, and more attractive for clinical use because of their high proliferative capacity, low immunogenicity, and lack of tumorigenicity<sup>19</sup>. However, the effects of soluble factors released from CH-MSCs and PL-MSCs on the growth and progression of CCA cells, as well as the molecular mechanisms that mediate these effects, are poorly understood.

Therefore, the present study aimed to investigate the effects and underlying molecular mechanisms of conditioned media prepared from human MSCs derived from chorion (CH-CM) and placenta (PL-CM) on the proliferation, migration and invasion of three human CCA cell lines (KKU100, KKU213A, and KKU213B). These findings serve as a basis for translational studies to explore the possibility of using MSCs in combination with other conventional treatments to improve the therapeutic outcome and increase the survival of CCA patients.

### Results

### Characteristics of human MSCs derived from chorion and placental tissues

CH-MSCs and PL-MSCs attached to the plastic surface presented a spindle-shaped morphology and exhibited adipogenic and osteogenic differentiation capacity, as demonstrated by oil red O and alizarin red S staining, respectively (Fig. 1A).

Flow cytometric analysis of cell surface antigens in CH-MSCs revealed high expression of the typical MSC markers CD73 (97.31 $\pm$ 1.39%), CD90 (95.11 $\pm$ 1.25%) and CD105 (95.25 $\pm$ 1.92%), and very low expression of the hematopoietic markers CD34 (2.31 $\pm$ 1.22%) and CD45 (4.73 $\pm$ 1.74%). Similarly to CH-MSCs, most PL-MSCs homogeneously expressed CD73 (99.04 $\pm$ 0.27%), CD90 (93.17 $\pm$ 0.92%) and CD105 (96.26 $\pm$ 2.06%) and rarely expressed CD34 (1.39 $\pm$ 1.13%) or CD45 (1.41 $\pm$ 1.23%) (Fig. 1B). These characteristics show that both the CH-MSCs and PL-MSCs established in this study presented all the typical characteristics of human MSCs.

### PL-CM and CH-CM suppress CCA cell proliferation

We first determined the effect of MSC-CM on CCA cell proliferation by treating three CCA cell lines, KKU100, KKU213A and KKU213B, with various concentrations of CH-CM and PL-CM for 24, 48, and 72 h. The findings indicated that CH-CM and PL-CM significantly decreased the relative number of all three CCA cell lines compared with that of the untreated control (0% MSC-CM) in a dose- and time-dependent manner (Fig. 2A,B). Notably, the highest concentration examined, 75% of either CH-CM or PL-CM, decreased the relative number of CCA cells by approximately 80% at 72 h compared with the untreated control (p<0.001; Fig. 2A,B). These results indicate that soluble factors secreted from both CH-MSCs and PL-MSCs strongly suppress CCA cell proliferation in a dose- and time-dependent manner.

### MSC-CM suppresses CCA cell migration and invasion

A scratch wound healing assay was performed to assess the effects of various concentrations of MSC-CM on the migration capacity of CCA cells. Similarly to their effects on CCA cell proliferation, CH-CM and PL-CM significantly decreased the migration of all three CCA cell lines in a dose- and time-dependent manner (Fig. 3A–D, Supplementary Fig. 1–3). Specifically, the suppressive effects of 75% CH-CM and PL-CM, the highest concentration examined, on CCA cell migration were observed as early as 6 h after treatment, and at the end of the migration assay, both CH-CM and PL-CM suppressed CCA cell migration by approximately 80% compared with the untreated control. As illustrated in Fig. 3B,D, the migration rates of KKU100 were substantially diminished from 23.84 to 2.16% (p=0.001), KKU213A from 77.83 to 12.25% (p<0.001), and KKU213B from 47.58 to 4.06% (p<0.001) after treatment with 75% CH-CM for 6 h. Similarly, treatment with 75% PL-CM for 6 h significantly reduced the migration rates of KKU100 from 24.61 to 6.01% (p=0.001), KKU213A from 77.90 to 1.98% (p<0.001), and KKU213B from 63.57 to 6.95% (p<0.001) in comparison to the control group. These findings suggest that soluble factors secreted by both CH-MSCs and PL-MSCs strongly inhibit CCA cell migration in a dose- and time-dependent manner.

Next, we investigated the effect of MSC-CM on CCA cell invasion using a transwell invasion assay. Similarly to the effects on CCA migration, both CH-CM and PL-CM significantly suppressed the invasion of the three CCA cell lines in a dose-dependent manner (Fig. 4A,B), with the highest concentration examined, 75% of either CH-CM or PL-CM, reducing invasion by more than 95% compared with that of the untreated controls (Fig. 4A,B). The invasion rate of KKU100 was reduced to 2.05% and 1.98% (p<0.001), KKU213A was reduced to 0.92% and 2.35% (p<0.001), and KKU213B was reduced to 1.31% and 2.69% (p<0.001), after being cultured with 75% CH-CM and 75% of PL-CM compared to the control, respectively. These findings indicate that soluble factors secreted by both CH-MSCs and PL-MSCs diminish CCA cell invasion in a dose-dependent manner.

### MSC-CM decreases the expression of mesenchymal markers in CCA cell lines

To investigate the mechanism by which CH-CM and PL-CM suppress the migration and invasion of CCA cells, the expression levels of genes and proteins involved in the epithelial-mesenchymal transition (EMT) process,

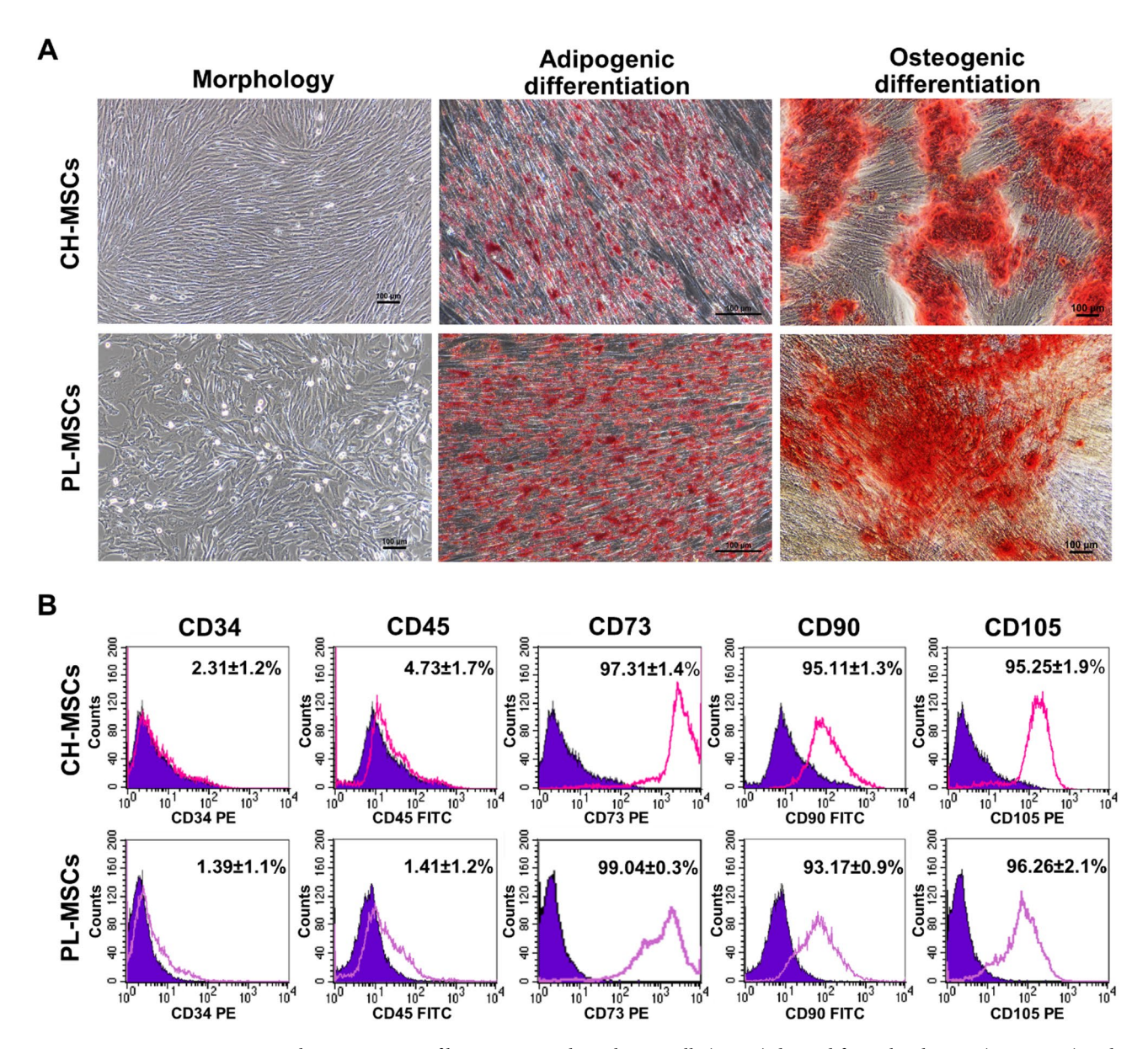
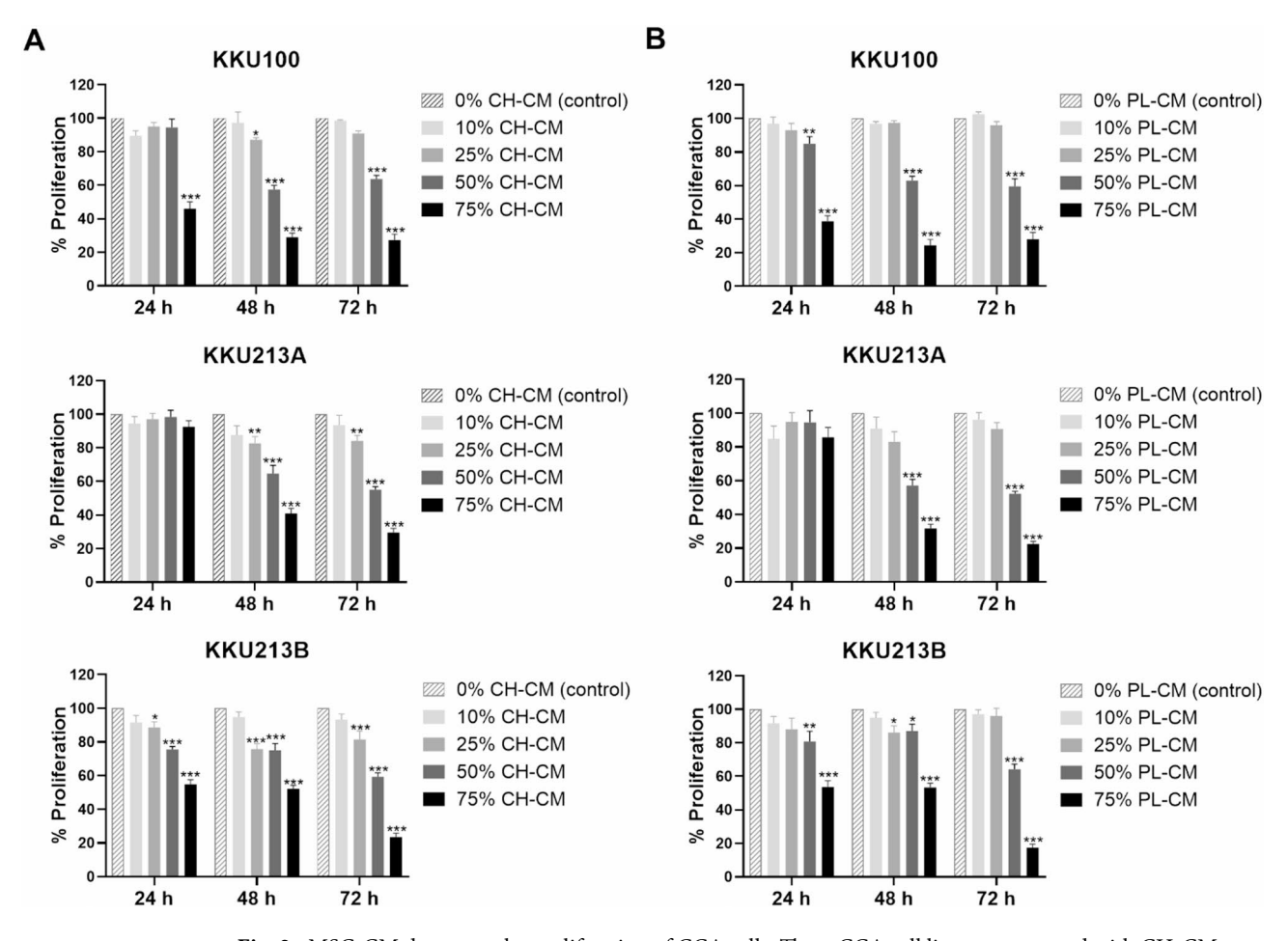


Fig. 1. Characterization of human mesenchymal stem cells (MSCs) derived from the chorion (CH-MSCs) and placenta (PL-MSCs). (A) CH-MSCs and PL-MSCs have a spindle-shaped morphology ( $10\times$  magnification). CH-MSCs and PL-MSCs can differentiate into adipocytes ( $20\times$  magnification) and osteocytes ( $10\times$  magnification), as determined by oil red O and alizarin red S staining, respectively. Scale bar =  $100~\mu$ m. (B) Immunophenotypes of CH-MSC and PL-MSC determined by flow cytometry.

including E-cadherin, N-cadherin, vimentin and MMP-2, were determined by immunocytochemistry, Western blotting and qRT-PCR. Immunofluorescence results indicated that CH-CM and PL-CM significantly decreased the expression of vimentin in CCA cells compared to their untreated counterparts in a dose-dependent manner (Fig. 5A). Quantitative analysis of vimentin staining using a microplate reader revealed that, compared with the untreated control, 75% CH-CM and PL-CM reduced vimentin protein expression in KKU213A and KKU213B cells by more than 70% (p<0.001; Fig. 5B). Similarly, 75% CH-CM and PL-CM also reduced the expression of the vimentin protein in KKU100 cells by approximately 40% (p=0.001, p<0.001), which was less pronounced than the effects on KKU213A and KKU213B cells (Fig. 5B).

Consistent with these findings, Western blot analysis also revealed that CH-CM and PL-CM significantly increased the expression level of E-cadherin, a cell-cell adhesion molecule, but significantly decreased the expression levels of N-cadherin and MMP-2, which play critical roles in inducing EMT and enhancing cell migration and invasion (Fig. 6A–D). The relative protein expression analysis revealed that treatment with 75% CH-CM and 75% PL-CM significantly enhanced E-cadherin expression in KKU100 (p=0.001, p<0.001), KKU213A (p=0.004, p=0.002), and KKU213B (p=0.020, p=0.014). Conversely, treatment with 75% CH-CM and 75% PL-CM significantly decreased N-cadherin expression in KKU100 (p=0.004, p<0.001), KKU213A (p<0.001, p=0.005), and KKU213B (p=0.023, p=0.003). Furthermore, treatment with 75% CH-CM and



**Fig. 2.** MSC-CM decreases the proliferation of CCA cells. Three CCA cell lines were treated with CH-CM or PL-CM at 0%, 10%, 25%, 50%, or 75%. Cell proliferation was determined by the CCK-8 assay at 24 h, 48 h, and 72 h after treatment. **(A)** CH-CM and **(B)** PL-CM significantly decreased the percentage of proliferating CCA cells compared with that of the untreated controls (0% MSC-CM). The data are represented as mean  $\pm$  SEM; n=3 for each group. \*p<0.05, \*\*p<0.01, \*\*\*p<0.01, \*\*\*p<0.001 vs. control.

75% PL-CM also significantly decreased MMP-2 expression in KKU100 (p<0.001, p<0.001), KKU213A (p<0.001, p<0.001), and KKU213B (p<0.001, p=0.049), respectively. Original uncropped blots are provided in Supplementary Fig. 4,5. These results suggest that CH-CM and PL-CM could inhibit the migration and invasion of CCA cells by suppressing their EMT.

### MSC-CM downregulates the activation of the PI3K/AKT pathway in CCA cell lines

The molecular mechanism underlying the suppressive effects of MSC-CM on several aspects of CCA cell tumorigenicity was further investigated by analyzing the activities of the PI3K/AKT and NF-κB signaling pathways, as well as the transcription factors that regulate the EMT process in CCA cells after treatment with MSC-CM. Gene expression analysis revealed that CH-CM and PL-CM significantly decreased the expression levels of the *PI3K*, *AKT* and *NF-kB2* genes in the three CCA cell lines (p < 0.05; Fig. 7). Notably, although 75% CH-CM and PL-CM significantly decreased the expression level of the *NF-kB1* gene in KKU213A (p = 0.046, p = 0.045) and KKU213B cells (p = 0.002, p < 0.001) compared with the untreated control, they did not significantly alter the expression of this gene in KKU100 cells (p > 0.999, p > 0.999) (Fig. 7).

Consistent with the results of the Western blot analysis of EMT proteins, the gene expression study showed that CH-CM and PL-CM significantly reduced the expression levels of the *ZEB1* and *ZEB2* genes (p<0.05), which are transcription factors that play important roles in the EMT process, as well as MMP-2 (p<0.05). Furthermore, MSC-CM decreased the expression levels of the proliferation-enhancing genes *CCND1* and *MYC* in the three CCA cell lines (Fig. 7; p<0.05).

Consistent with the gene expression results, Western blot analysis revealed that 75% CH-CM and 75% PL-CM decreased the levels of phosphorylated PI3K protein (p-PI3K) and phosphorylated AKT protein (p-AKT) in the three CCA cell lines compared with those in the untreated controls (Fig. 8A,C). Consistent with this, treatment with 75% CH-CM and 75% PL-CM significantly reduced the phosphorylated PI3K (p-PI3K) to total PI3K ratio in KKU100 (p = 0.003 and p < 0.001), KKU213A (p < 0.001 and p = 0.008), and KKU213B (p = 0.001 and p < 0.001) compared to the untreated control (Fig. 8B,D). Similarly, treatment with 75% CH-CM and 75% PL-CM also significantly decreased the phosphorylated AKT (p-AKT) to total AKT ratio in KKU100 (p < 0.001

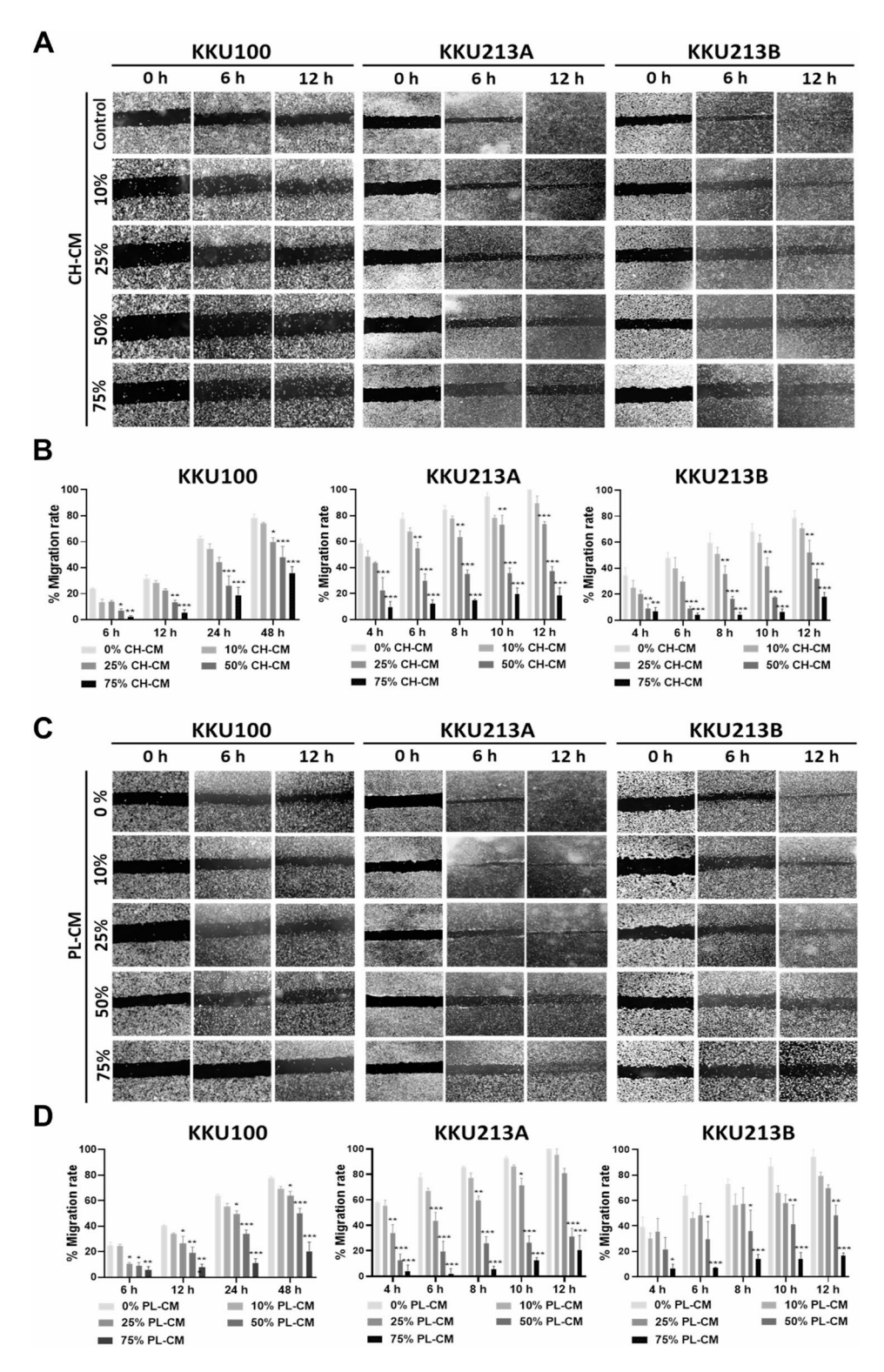


**Fig. 3.** MSC-CM inhibits CCA cell migration. CCA cell cultures were scratched and treated with various concentrations (0%, 10%, 25%, 50% and 75%) of (**A**) CH-CM or (**C**) PL-CM. Phase contrast microscopy was used to measure the migration distances at various time points. (**B**) CH-CM and (**D**) PL-CM considerably reduced the migration rate of CCA cells compared with that of the untreated controls (0% MSC-CM). Data are represented as mean  $\pm$  SEM; n=3 for each group. \*p<0.05 vs. control, \*\*p<0.01 vs. control, \*\*\*p<0.001 vs. control.

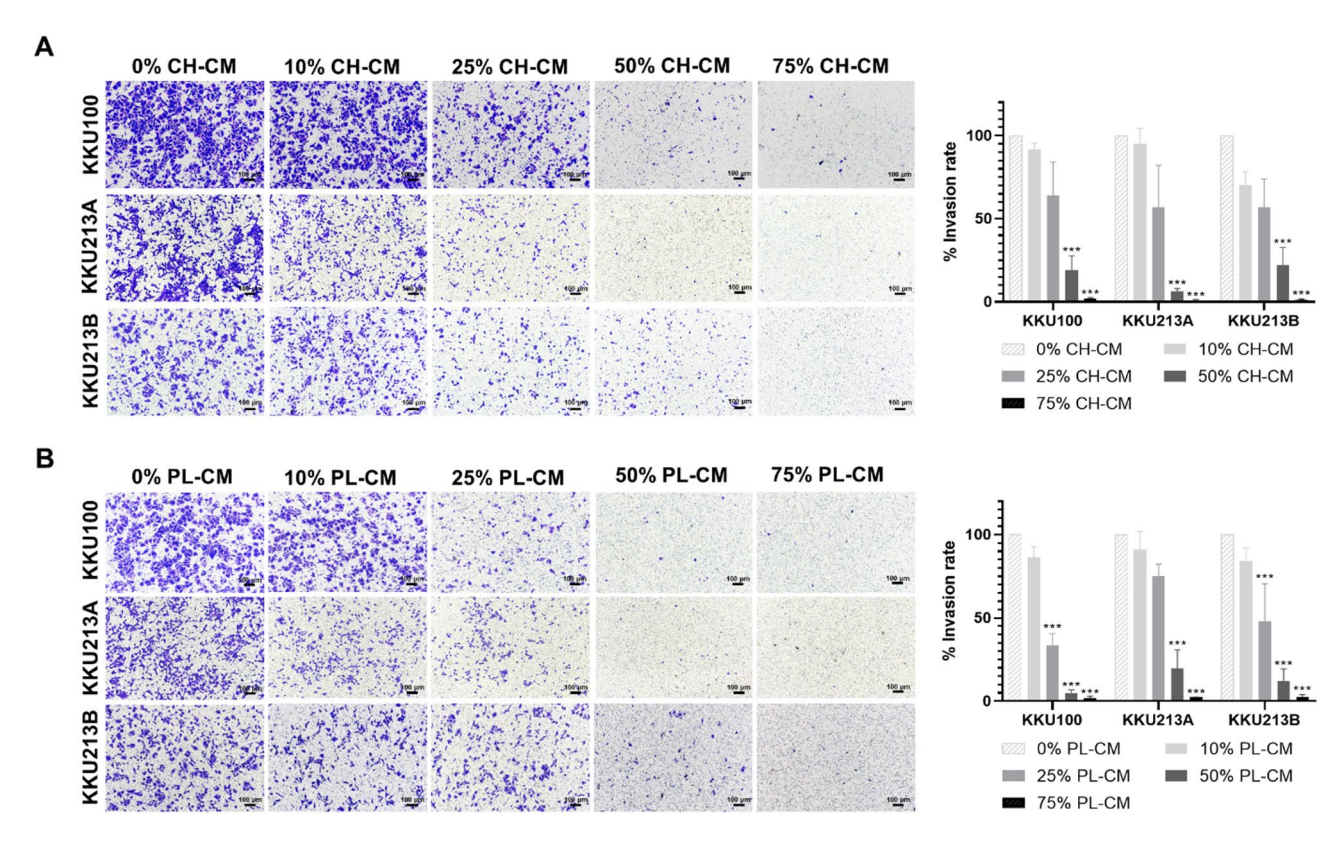


**Fig. 4.** MSC-CM inhibits CCA cell invasion. CCA cells were treated with various concentrations (0%, 10%, 25%, 50% and 75%) of (**A**) CH-CM or (**B**) PL-CM. The invading cells (present on the lower side of the transwell membranes) were stained and counted under an inverted microscope (10X). Scale bar = 100  $\mu$ m. (**A**) CH-CM and (**B**) PL-CM significantly decreased CCA cell invasion compared with that of the untreated control (0% MSC-CM). The data are presented as the mean  $\pm$  SEM; n=3 for each group. \*p<0.05 vs. control, \*\*p<0.01 vs. control, \*\*\*p<0.001 vs. control.

and p=0.003), KKU213A (p<0.001 and p=0.040), and KKU213B (p<0.001 and p=0.020) compared to the untreated control (Fig. 8B,D). The p-PI3K/PI3K and p-AKT/AKT ratios in CCA cells treated with 75% CH-CM and 75% PL-CM were similar to those treated with LY294002, a pan-PI3K inhibitor (Fig. 8A-D). Original uncropped blots are provided in Supplementary Fig. 6–8. Together, these findings demonstrate that CH-CM and PL-CM exert their antitumor effects on CCA cells by inhibiting the PI3K/AKT signaling pathway in these cells.

### CH-CM and PL-CM inhibit CCA cell migration and invasion by inhibiting PI3K/AKT signaling

To confirm the roles of the PI3K/AKT signaling pathway in CCA cell migration and invasion, CCA cells were treated with LY294002, a pan-PI3K inhibitor, before being subjected to wound healing and transwell invasion assays. The results of the wound healing assay revealed that 75% CH-CM, 75% PL-CM, LY294002, or their combination significantly reduced the migration rate of the three CCA cell lines compared with that of the untreated control (0% MSC-CM) (p < 0.01, p < 0.001; Fig. 9A,B). Similarly, the results of the transwell invasion assays revealed that 75% CH-CM and 75% PL-CM significantly reduced the percentage of invasion rate, similar to those treated with LY294002 in CCA cell lines compared with the untreated control (0% MSC-CM) (p < 0.001; Fig. 10A,B). These findings indicate that CH-CM and PL-CM could suppress the migration and invasion of CCA cells at least partially by inhibiting PI3K/AKT signaling in these cells.

### Discussion

Cholangiocarcinoma is a highly aggressive cancer that responds poorly to most conventional treatments, resulting in a very low survival rate<sup>20</sup>. Consequently, the development of a new therapeutic approach, in which mesenchymal stem cell therapy is considered a promising treatment, is necessary<sup>21</sup>. Mesenchymal stem cells (MSCs) are multipotent adult stem cells with self-renewal capacity, multilineage differentiation capacity, and the ability to secrete many therapeutically useful factors<sup>22</sup>. MSCs can be isolated from many adult tissues, including bone marrow<sup>23</sup>, adipose tissue<sup>24</sup>peripheral blood<sup>25</sup>, and postnatal tissues such as the placenta, chorionic membrane, amniotic membrane, and umbilical cord<sup>26</sup>.

Although bone marrow-derived mesenchymal stem cells (BM-MSCs) are the most widely used source of MSCs in various clinical applications, including regenerative medicine, tissue engineering, and cancer treatment<sup>27,28</sup>, their therapeutic utility is limited by their invasive harvesting procedure, poor cell yield, limited proliferation and diminished differentiation capacity, particularly in aged donors<sup>29,30</sup>. Therefore, human MSCs derived from

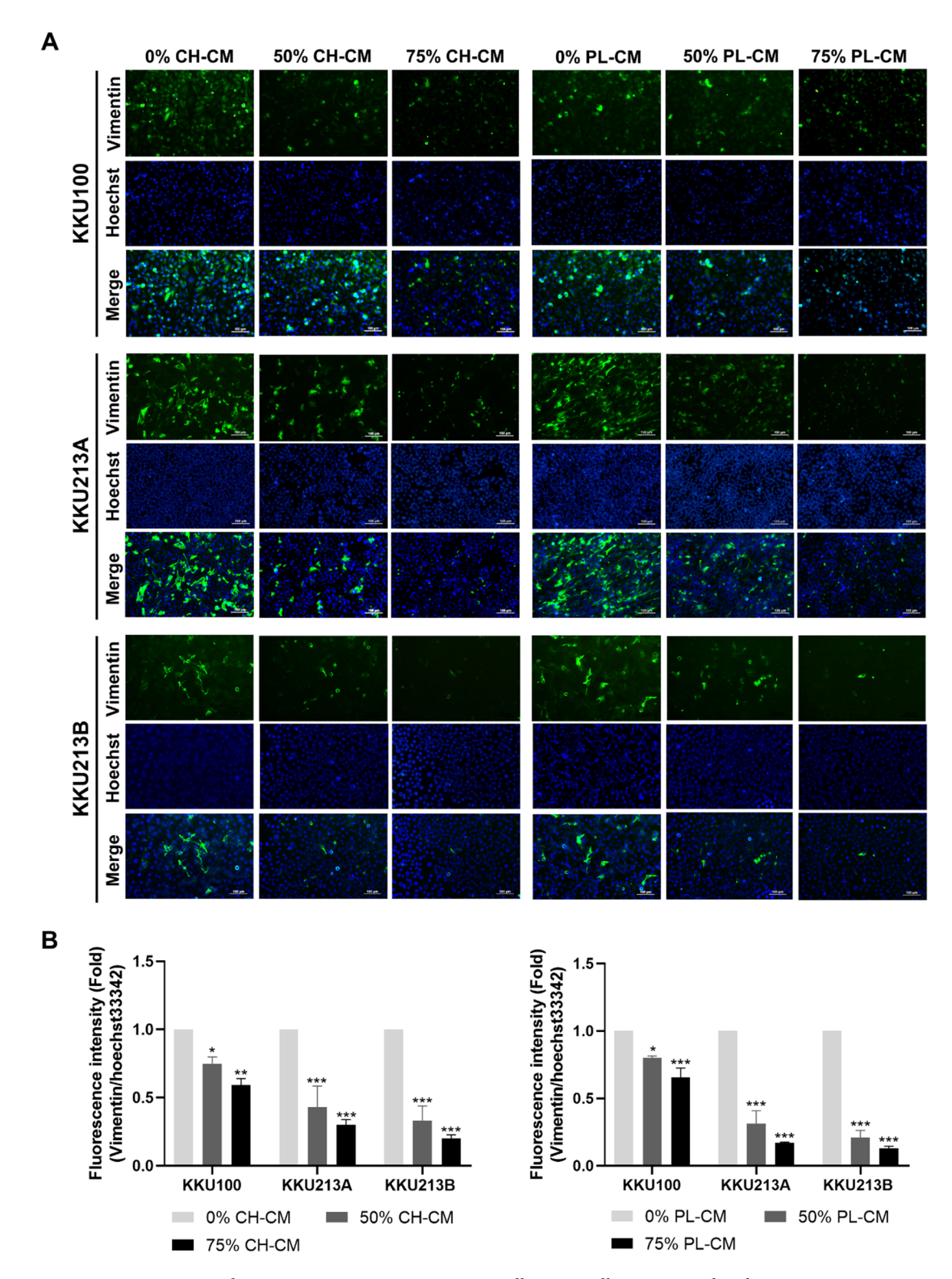


**Fig. 5.** MSC-CM reduces vimentin expression in CCA cells. CCA cells were treated with CH-CM or PL-CM at 0%, 50%, or 75% for 16 h and then stained with an anti-vimentin antibody (green fluorescence). The nuclei were counterstained with Hoechst 33342 (blue fluorescence). (**A**) Fluorescence microscopy analysis revealed a decrease in green fluorescence (vimentin) in CCA cells after treatment with 50% or 75% CH-CM or PL-CM. Scale bar = 100  $\mu$ m. (**B**) Vimentin staining was quantified using a fluorescence microplate reader. The results showed that 50% and 75% CH-CM and PL-CM significantly decreased the fluorescence ratio of vimentin/ Hoechst 33342 in CCA cells compared with that of the untreated control (0% MSC-CM). Data are represented as mean  $\pm$  SEM; n=3 for each group. \*p<0.05 vs. control, \*\*p<0.01 vs. control, \*\*\*p<0.001 vs. control.

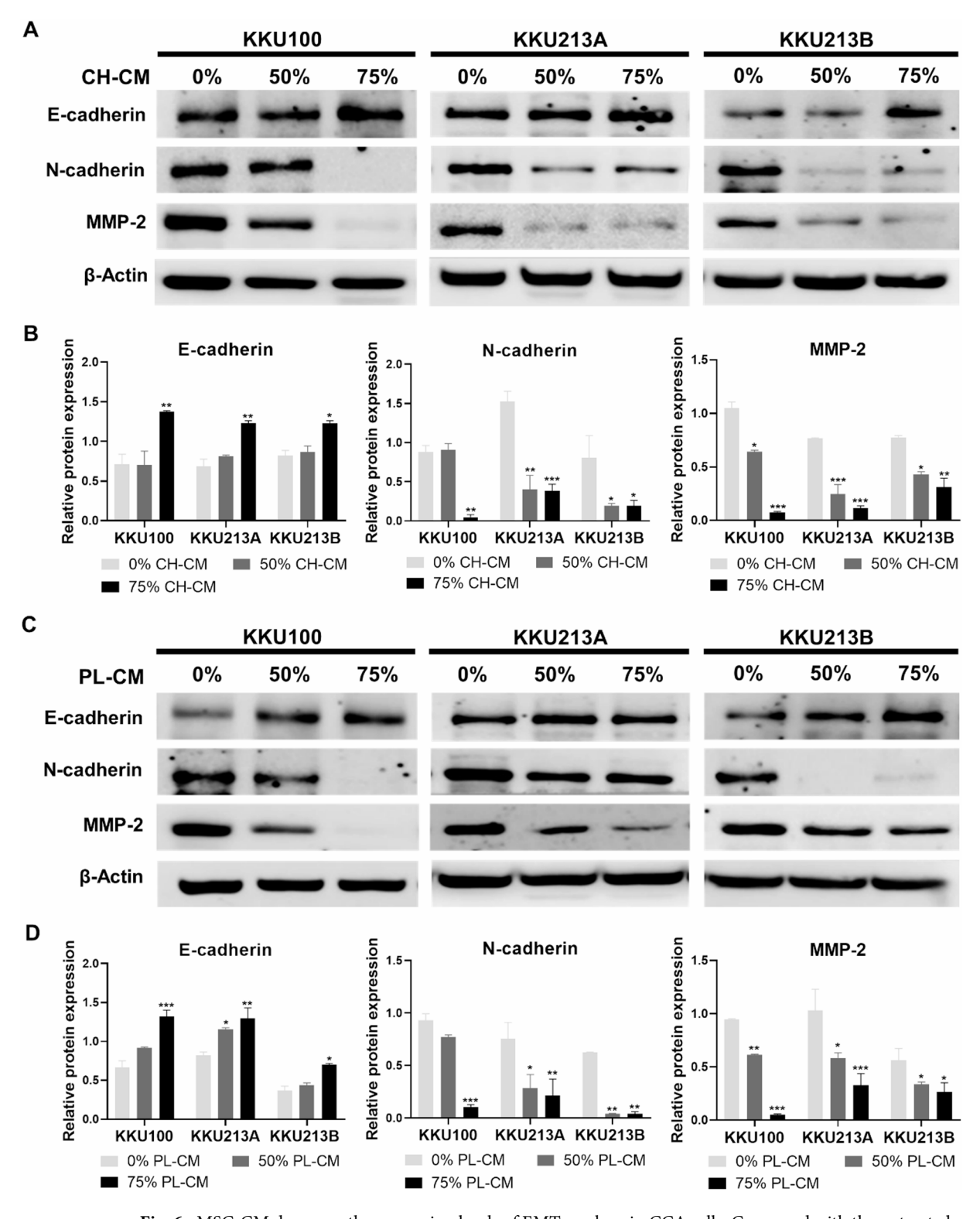


**Fig. 6.** MSC-CM decreases the expression levels of EMT markers in CCA cells. Compared with the untreated control (0% MSC-CM), the three CCA cell lines treated with (**A,B**) CH-CM or (**C,D**) PL-CM for 16 h presented increased expression of E-cadherin and decreased expression of the EMT markers N-cadherin and MMP-2. The uncropped blots of (**A**) and (**C**) are presented in Supplementary Fig. 4, 5, respectively. Data are represented as mean  $\pm$  SEM; n=3 for each group. \*p<0.05 vs. control, \*\*\*p<0.01 vs. control, \*\*\*p<0.001 vs. control.

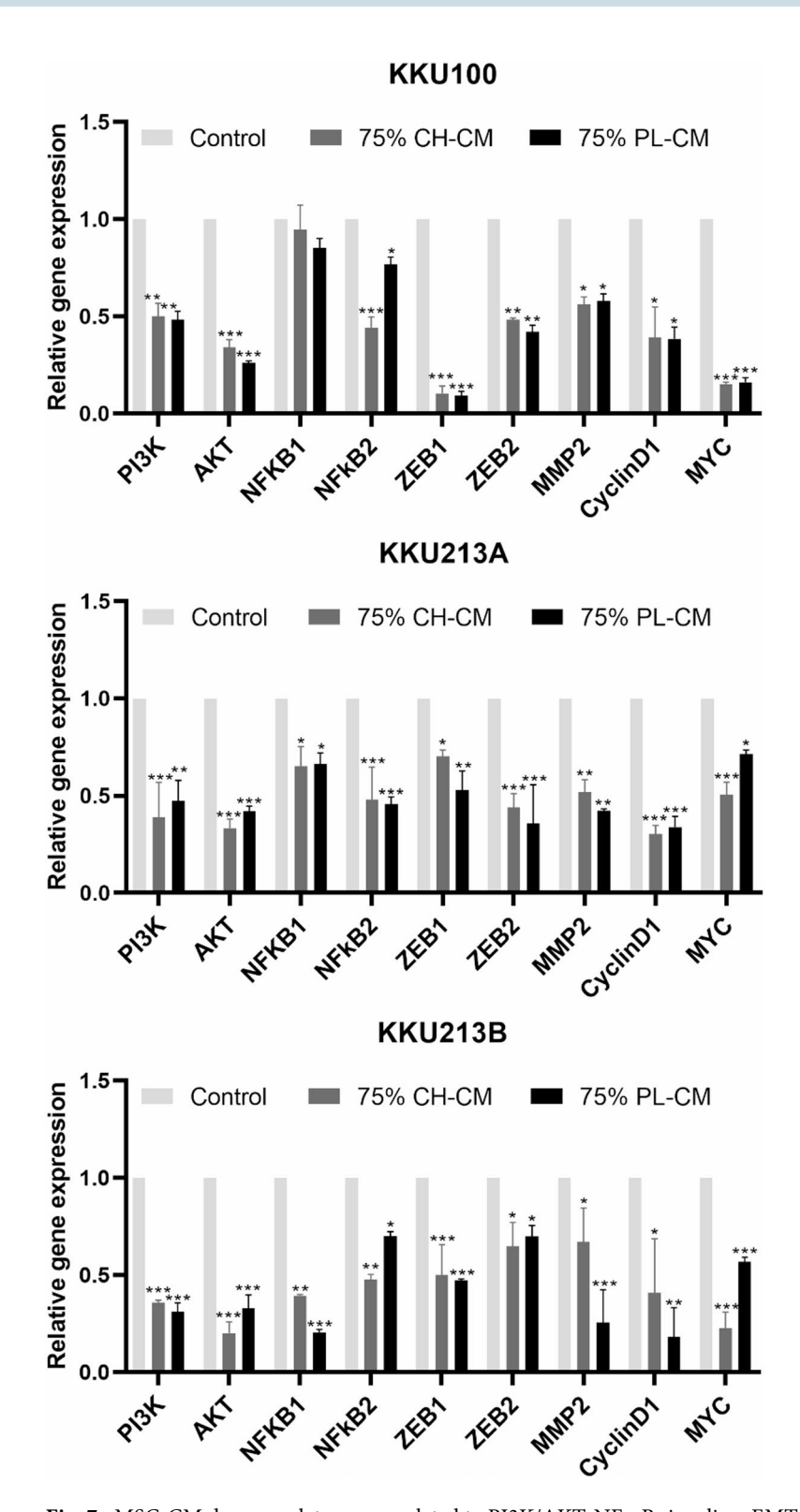


**Fig.** 7. MSC-CM downregulates genes related to PI3K/AKT, NF- $\kappa$ B signaling, EMT process and cell cycle control in CCA cells. CCA cells were treated with 75% CH-CM or 75% PL-CM for 16 h. CCA cells treated with DMEM + 10% FBS served as controls. Relative gene expression analysis revealed that CH-CM and PL-CM significantly decreased the expression levels of *PI3K*, *AKT*, *NF-kB1*, *NF-kB2*, *ZEB1*, *ZEB2*, *MMP-2*, *CCND1* and *MYC* in CCA cells compared with those in untreated controls (0% MSC-CM). Data are represented as mean  $\pm$  SEM; n=3 for each group. \*p<0.05 vs. control, \*\*p<0.01 vs. control, \*\*\*p<0.001 vs. control.

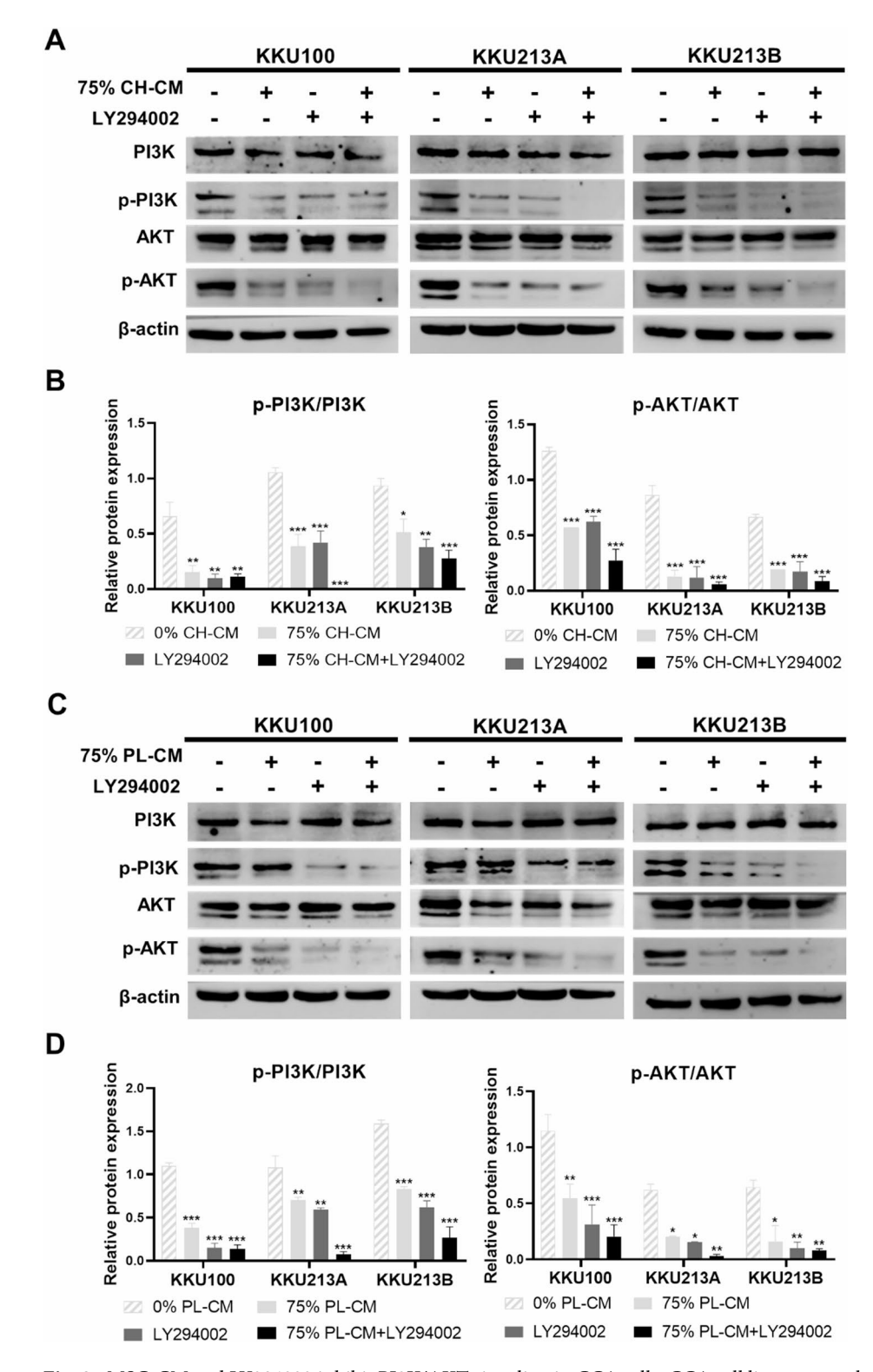


**Fig. 8.** MSC-CM and LY294002 inhibit PI3K/AKT signaling in CCA cells. CCA cell lines were cultured with 75% CH-CM, 75% PL-CM, 20 μM LY294002, or a combination of these for 16 h. Western blot analysis showed that CH-CM, PL-CM or LY294002 significantly reduced the p-PI3K/PI3K and p-AKT/AKT ratios in all CCA cells, and the combination enhanced the inhibitory effect on PI3K and AKT activation compared with that of the untreated control (0% MSC-CM). The uncropped blots are presented in Supplementary Fig. 6–8. Data are represented as mean  $\pm$  SEM; n=3 for each group. \*p<0.05 vs. control, \*\*p<0.01 vs. control, \*\*p<0.001 vs. control.

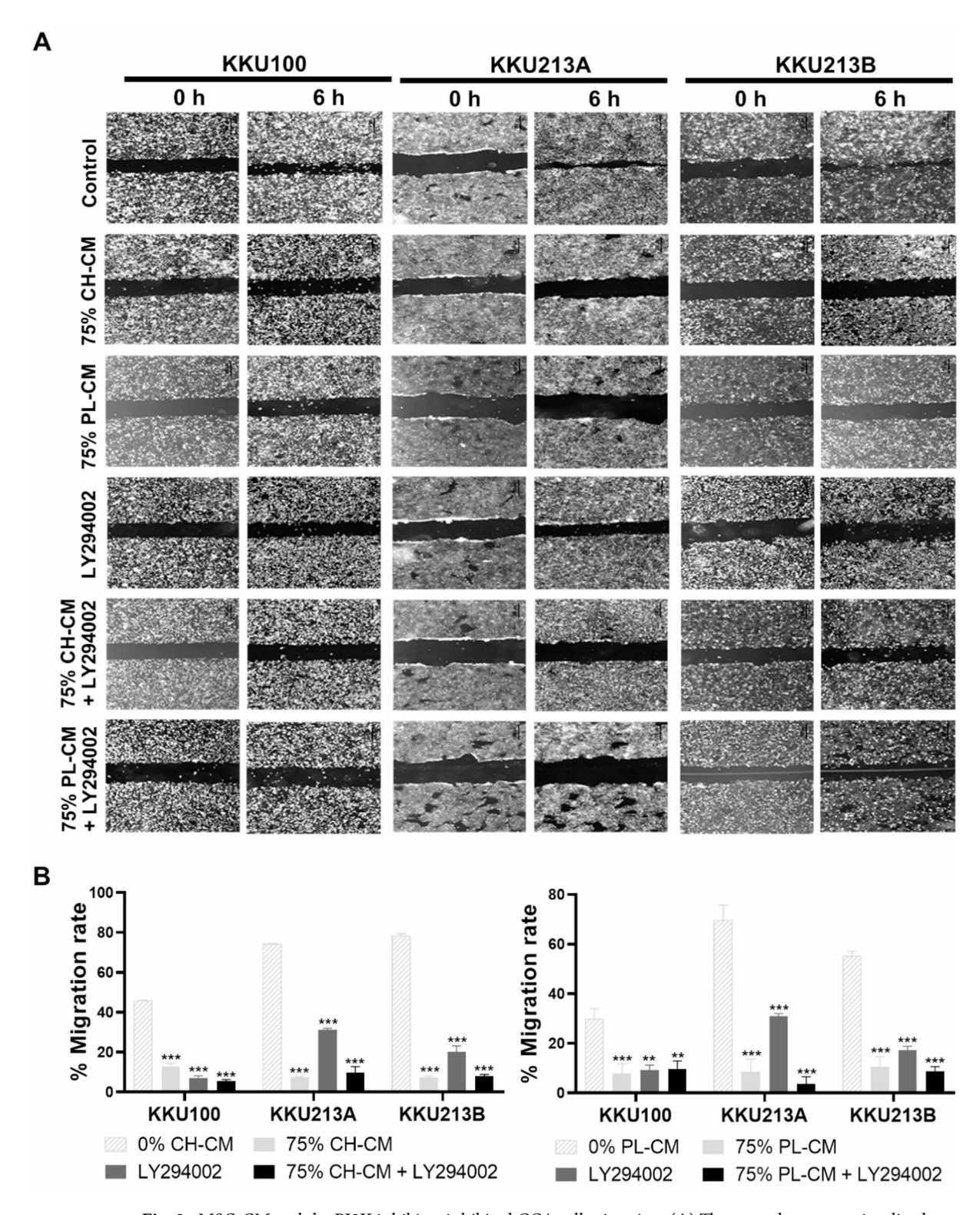


**Fig. 9.** MSC-CM and the PI3K inhibitor inhibited CCA cell migration. (**A**) The wound area was visualized and measured at 0 h and 6 h after culture with 75% CH-CM, 75% PL-CM, 20 μM LY294002 or a combination. (**B**) Quantification of the migration rate revealed that CH-CM, PL-CM and 20 μM LY294002 independently suppressed wound closure by significantly decreasing the percentage of migration rate of CCA cells compared with the untreated control (0% MSC-CM). Data are represented as mean ± SEM; n = 3 for each group. \*\*p < 0.01 vs. control, \*\*\*p < 0.001 vs. control.

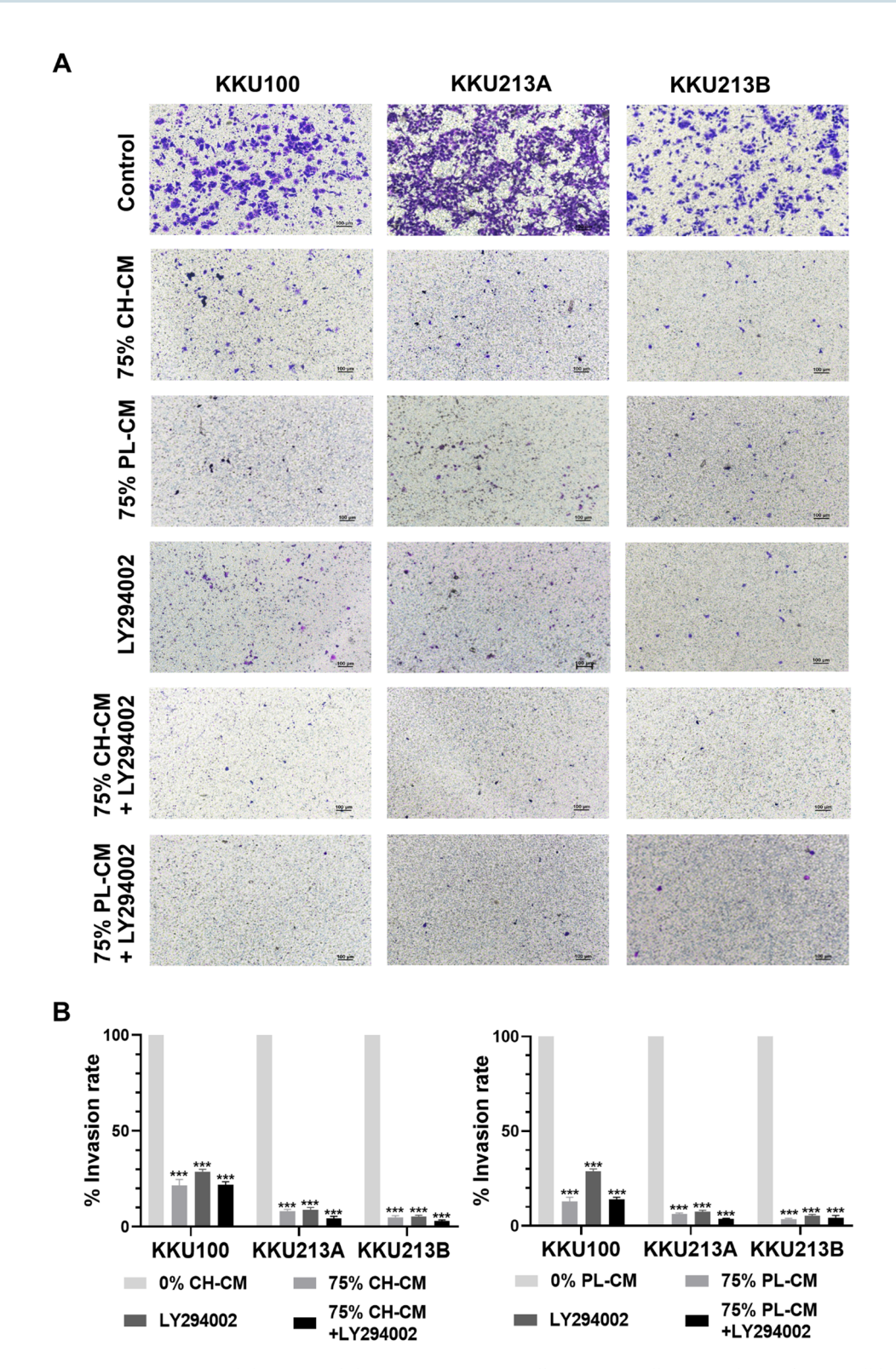


Fig. 10. MSC-CM and the PI3K inhibitor suppress CCA cell invasion. Following culture of CCA cell lines with MSC-CM,  $20~\mu$ M LY294002 or a combination of these for 16 h, the results of the transwell assays revealed a significant decrease in CCA cell invasion compared with that of the untreated control (0% MSC-CM). (A) Imaging of the lower surface of the transwell membranes. Scale bar =  $100~\mu$ m. (B) Quantification of the invasion rate. Data are represented as mean  $\pm$  SEM; n=3 for each group. \*\*\*p<0.001 vs. control.

other tissues, especially the chorion and placenta (CH-MSCs and PL-MSCs), which can be obtained in large numbers via noninvasive procedures, are considered the preferred options for clinical applications. These CH-MSCs and PL-MSCs have been shown to have many clinically useful properties, including high cell viability, high proliferation capacity, and low immunogenicity, and have great paracrine effects on the repair of injured and ischemic tissues<sup>31,32</sup>. Furthermore, previous research has shown that MSCs can migrate toward cancer tissue, a property called tumor tropism, and release various cytokines, growth factors and extracellular matrix proteins with both protumorigenic and antitumorigenic properties<sup>33,34</sup>.

In addition to MSC transplantation, cell-free MSC-CM has recently been considered a safer option for MSC-based therapy because of its easier production, better quality control, ease of delivery to various target tissues, and fewer adverse effects than those of cell transplantation<sup>35</sup>. Although several previous studies have demonstrated the antitumor effects of MSC-CM in various types of cancer, including non-small cell lung cancer<sup>36</sup>, glioblastoma<sup>37</sup> and malignant melanoma<sup>38</sup>, the effects of CM derived from CH-MSCs and PL-MSCs on CCA cells have not yet been fully investigated.

To ensure sterility and enhance storage stability, the hMSC-derived CMs utilized in this study were subjected to filter sterilization and lyophilization. It should be noted that sterilization through  $0.22\,\mu m$  pore filters, although widely employed, may exclude certain large macromolecules, such as large protein complexes and extracellular vesicles (EVs), potentially diminishing the CM potency. Similarly, lyophilization (freeze-drying), a prevalent method for preserving CMs by eliminating water content while preserving their bioactivity, could result in denaturation and aggregation of certain bioactive proteins within CMs. To prevent further loss of activity due to repeated freeze-thaw cycles, the CM was aliquoted into small volumes for a single use.

Here we demonstrated that CH-CM and PL-CM strongly inhibited the proliferation, migration and invasion of three different human CCA cell lines, including a low-invasive, poorly differentiated extrahepatic CCA cell line (KKU100), a highly invasive, poorly differentiated intrahepatic CCA cell line (KKU213A) and a low invasive, well-differentiated intrahepatic CCA line (KKU213B). The suppressive effect of conditioned medium derived from human chorion and placental amniotic membrane derived hMSCs (CH-CM and PL-CM) on cancer cell growth is consistent with our previous research showing that these conditioned media inhibit cancer growth by promoting apoptosis of CCA cells through the induction of mitochondria-mediated caspase activity<sup>39,40</sup>. Furthermore, these findings are consistent with previous research showing that CM derived from human umbilical cord-derived MSCs, another widely used type of gestational tissue-derived MSC, suppresses the growth and migration of human hepatocellular carcinoma and lung adenocarcinoma<sup>41</sup>. However, the findings of the present study contrast with those of some other previous studies showing that CM derived from bone marrow-derived MSCs increases the proliferation, migration and invasion of head and neck cancer and colorectal cancer<sup>42,43</sup>. This discrepancy is likely due to differences in the source of MSCs, the type of cancer and the experimental methodologies used in each study.

The epithelial-mesenchymal transition (EMT) represents a critical mechanism in tumor metastasis and is a major contributor to tumor-related mortality in CCA patients<sup>44</sup>. The EMT is a complex process of transforming an epithelial into a mesenchymal cell phenotype, which is characterized by the loss of E-cadherin-mediated cell-cell adhesion and an increase in the expression levels of mesenchymal markers such as vimentin and N-cadherin, a mesenchymal cytoskeleton and adhesion molecule, which are crucial for cell motility and invasion. Additionally, there is an increase in the production of MMP-2, a proteolytic enzyme associated with the degradation of the extracellular matrix, which greatly facilitates cancer cell migration and invasion<sup>45,46</sup>. Our study demonstrated that both CH-CM and PL-CM suppressed epithelial-to-mesenchymal transition (EMT) by decreased the expression of mesenchymal markers (vimentin, N-cadherin, and MMP-2) and concurrently increasing the expression of the epithelial marker (E-cadherin) in CCA cells. While the EMT suppression correlated with a decrease in CCA cell migration and invasion, the direct causal relationship between this EMT suppression and the observed decrease in migratory/invasive activity of CCA cells following hMSC-CM treatment remains inconclusive.

EMT is a complex process regulated by multiple signaling pathways, including transforming growth factor-beta (TGF-β), fibroblast growth factor (FGF), epidermal growth factor (EGF), Wnt/β-catenin, Notch, and PI3K/AKT signalings. Among these pathways, the PI3K/AKT pathway holds significant importance due to its extensive interactions with NF-kB, MYC, cyclin D1, and MMP-2, which play pivotal roles in regulating the growth, migration, invasion, and metastasis of diverse cancer types<sup>47-49</sup>, especially CCA<sup>11,50</sup>. Consistent with these findings, our study demonstrated that CH-CM and PL-CM strongly inhibited the PI3K/AKT signaling pathway in CCA cells, as demonstrated by decreases in the p-PI3K/PI3K and p-AKT/AKT ratios, as well as decreases in the expression levels of its target genes, *NF-kB1*, *NF-kB2*, *MYC*, *CCND1* and *MMP-2*. Furthermore, CH-CM and PL-CM also suppressed the expression of zinc finger E-box binding homeobox-1 (ZEB1) and zinc finger E-box binding homeobox-2 (ZEB2), which are transcription factors that promote EMT and increase cancer cell migration. Based on these evidence, it is plausible that the suppression of EMT could contribute to the observed reduction in CCA cell migration and invasion after treatment with hMSC-CM. Given that EMT is regulated by the PI3K/AKT pathway, it is also conceivable that hMSC-CM might suppress EMT by inhibiting PI3K/AKT signaling in CCA cells.

Our results revealed that CH-CM and PL-CM significantly reduced CCA cell migration and invasion in a similar manner to LY294002, a pan-PI3K inhibitor that significantly reduces the p-PI3K/PI3K and p-AKT/AKT ratios in CCA cells. These findings indicate that PI3K/AKT signaling plays an important role in the regulation of CCA migration and invasion and that CH-CM and PL-CM can suppress the migration and invasion of CCA cells, at least partially, by inhibiting PI3K/AKT signaling in these cells. Our findings are consistent with those of previous studies showing that MSCs derived from bone marrow and the umbilical cord suppress the proliferation, migration and invasion of glioma and CCA cells by inhibiting the PI3K/AKT signaling pathway and suppressing EMT in these cells<sup>51,52</sup>. Nevertheless, the rescue experiment by overexpressing AKT is required to definitively confirm the roles of PI3K/AKT signaling in mediating the effects of hMSC-CM in CCA cells.

Notably, the suppressive effects of CH-CM and PL-CM on the migration of KKU213A and KKU213B cells are even greater than those of LY294002 alone, and the addition of LY29400 did not further increase the suppressive effects of CH-CM and PL-CM on the three CCA cell lines. This observation suggests that soluble factors derived from both CH-MSCs and PL-MSCs can suppress CCA migration through other additional signaling pathways, such as JAK2/STAT3<sup>53</sup> and Wnt/ $\beta$ -catenin<sup>54</sup> pathways, which have been shown to play important roles in CCA progression<sup>55,56</sup>.

Previous studies have identified several hMSC-derived anti-tumorigenic factors. For instance, IGF-1R, as well as exosomes containing miR-22-3p and miR-30b-5p, have been shown to inhibit tumor growth, invasion, and promote apoptosis through the suppression of the PI3K/AKT pathway<sup>15,57,58</sup>. Similarly, miR-3940-5p, miR-150, and miR-133b which target Integrin  $\alpha$ 6, IGF2BP, and EZH2, respectively, decrease tumor cell proliferation, migration, invasion by suppressing EMT<sup>59-61</sup>. Furthermore, TRAIL and interferons  $\beta$  (IFN- $\beta$ ) also contribute to tumor suppression by inducing cancer cell apoptosis<sup>62,63</sup>. Tissue inhibitor of metalloproteinases-1 and -2 (TIMP-1 and TIMP-2) have also been reported to inhibit cancer cell migration and invasion by suppressing the activity of MMP-1, MMP-2, and MMP-9<sup>64</sup>. Many of these molecules have been detected in MSC-derived exosomes, EVs, or conditioned media (CM) and are considered strong candidates for the anti-metastatic effects observed in this study. While our findings support the anti-tumorigenic effects of MSC-CM against CCA cells, further research is necessary to identify the specific molecules involved and confirm their impact on important signaling pathways, particularly the PI3K/AKT pathway.

In conclusion, the present study demonstrates that soluble factors secreted from CH-CM and exert anticancer effects on human CCA cell migration and invasion by inhibiting the EMT process, most likely through suppression of the PI3K/AKT signaling pathway. These findings suggest that soluble factors derived from CH-MSCs and PL-MSCs could be used in combination with other conventional treatments to improve therapeutic outcomes and increase survival in advanced-stage CCA patients.

### Methods

### Culture of cholangiocarcinoma (CCA) cell lines

Three human CCA cell lines, KKU100, KKU213A, and KKU213B, were originally derived from Thai patients with CCA. Written informed consent was obtained from each patient, following the protocol established by Prof. Banchob Sripa at Khon Kaen University<sup>65,66</sup>. KKU100 originates from a low-invasive and poorly differentiated extrahepatic CCA. KKU213A is derived from a highly invasive and poorly differentiated intrahepatic CCA, whereas KKU213B is a low-invasive and well-differentiated intrahepatic CCA cell line. KKU100 and KKU213B were maintained in Ham's F12 media supplemented with 10% (v/v) fetal bovine serum (FBS), 1% (v/v) antibiotic-antimycotic mixture and 1% (v/v) L-glutamine. KKU213A cells were maintained in high-glucose DMEM supplemented with 10% FBS, 1% antibiotic-antimycotic mixture and 1% L-glutamine. The use of cholangiocarcionoma cell lines was approved by the Institute Biosafety Committee of Thammasat University (Permission Number 039/2564).

### Isolation and culture of human chorion- and placenta-derived MSCs (CH-MSCs and PL-MSCs)

The chorion membrane and placental tissues were obtained from healthy full-term newborns (n=3) and cut into small pieces (approximately  $2 \times 2$  mm³ each). The tissues were then washed twice with phosphate-buffered saline (PBS) supplemented with 1% penicillin/streptomycin, centrifuged at  $500\times g$  for 5 min to remove the remaining blood, and digested with 0.5% (w/v) trypsin-EDTA for 2 h at 37 °C with shaking. After incubation, the isolated cells were washed twice with PBS and seeded in a 25 cm² flask with DMEM supplemented with 10% FBS, 1% penicillin/streptomycin and 1% L-glutamine at 37 °C in a humidified atmosphere containing 5% CO₂. The medium was replaced every three days until the cells reached 80% confluence. The protocol of the study was reviewed and approved by the Human Ethics Committee of Thammasat University No. 1 (Faculty of Medicine) (066/2021). Informed consent was obtained from all subjects and/or their legal guardian(s). The study was conducted according to the guidelines of the Declaration of Helsinki and the ICH Good Clinical Practice Guidelines and approved by the Thammasat University Ethics Committee.

### Characterization of CH-MSCs and PL-MSCs

At passages 3–4, the isolated cells were characterized by typical MSC markers defined by the International Society for Cellular Therapy (ISCT)<sup>67</sup>, including spindle-shaped morphology, multilineage-differentiation capacity and surface marker expression.

The adipogenic and osteogenic differentiation capacities were determined by culturing the cells in adipogenic differentiation medium (DMEM supplemented with 10% FBS, 2 mM L-glutamine, 0.5 mM isobutyl methylxanthine, 1  $\mu$ M dexamethasone, 10  $\mu$ M insulin and 100  $\mu$ M indomethacin) or osteogenic differentiation medium (DMEM supplemented with 10% FBS, 100 nM dexamethasone, 10 mM  $\beta$ -glycerophosphate and 50  $\mu$ g/ml ascorbic acid). After 4 weeks of induction, the cells were stained with oil red O or alizarin red S to detect lipid droplets in MSC-derived adipocytes and calcium deposition in MSC-derived osteocytes, respectively.

The expression of surface marker proteins was determined by labeling cells with fluorescein isothiocyanate (FITC)-conjugated antibodies against CD34, CD73 and CD105, as well as phycoerythrin (PE)-conjugated antibodies against CD45 and CD90. IgG was used as an isotype control. The cells were then analyzed by flow cytometry (FACSCalibur™, Becton Dickinson, USA) using CellQuest\* version 3.3 software (Becton Dickinson, USA) licensed to Thammasat University (https://timothyspringer.org/sites/g/files/omnuum3646/files/tas/files/c ellquest-softwarereference.pdf).

### Conditioned medium preparation

CH-MSCs or PL-MSCs at passages 3–4 were cultured until their density reached at least 80% confluence. The cells were then washed twice with PBS and incubated with serum-free high-glucose DMEM for another 24 h to generate conditioned medium (CM). Following a 24-hour incubation period, the conditioned medium (CM) was collected and centrifuged at 500 g for 5 min. The supernatant was subsequently sterilized by filtering through a 0.22  $\mu$ m pore size membrane. This filtration removed any remaining cell debris while retaining bioactive molecules smaller than the membrane pore size, including small extracellular vesicles. The CM was then concentrated by lyophilization, aliquoted, and stored at -80 °C until further use. Finally, the concentrated CM was diluted with Ham's F12+10% FBS or DMEM+10% FBS to generate various concentrations of CM.

### **CCK-8** proliferation assay

A total of  $9 \times 10^3$  KKU100 cells/cm²,  $4.5 \times 10^3$  KKU213A cells/cm² or  $4.5 \times 10^3$  KKU213B cells/cm² were seeded in 96-well plates and treated with 10%, 25%, 50% or 75% CH-CM or PL-CM to determine the effect of CM derived from MSCs (MSC-CM) on CCA cell proliferation. Cell proliferation was determined at 24, 48 and 72 h after treatment using the Cell Counting Kit-8 (CCK-8; Dojindo Molecular Technologies, Inc., Gaithersburg, MD, USA) according to the manufacturer's instructions. Briefly, the cells were incubated with 10  $\mu$ l of CCK-8 solution for 4 h at 37 °C, and the absorbance was measured at 450 nm using a microplate reader (BioTex, USA). The percentage of cell proliferation was calculated from the optical density values of each sample and of the untreated control (0% MSC-CM).

### Migration assay

A scratch wound healing assay was used to examine the effects of CH-CM and PL-CM on the migration of CCA cells. CCA cells were seeded in 24-well plates at a density of  $2.5 \times 10^5$  cells/cm<sup>2</sup>. When the cell density reached 80% confluence, a sterile 200 µl pipette tip was used to scrape the cell surface to create a wound area. The cells were then gently washed with PBS and incubated with 10%, 25%, 50% and 75% CH-CM or PL-CM diluted with DMEM+10% FBS. Migration distances were measured at 0, 4, 6, 8, 10, and 12 h by phase contrast microscopy. The migration of CCA cells was calculated using the following formula: Migration rate (%) = [(Distances at 0 h - Distances at the time point)/Distances at 0 h]  $\times$  100. CCA cells treated with DMEM+10% FBS served as controls.

### Invasion assay

The invasion of CCA cells was evaluated via transwells with a 0.8  $\mu$ m pore size (Corning, NY). A total of  $6\times10^4$  KKU100 cells,  $2\times10^4$  KKU213A cells and  $2\times10^4$  KKU213B cells were resuspended in 200  $\mu$ l of FBS-free DMEM and seeded in the upper chamber of a transwell plate coated with 0.4 mg/ml Matrigel. The lower chamber was then filled with 600  $\mu$ l of 10–75% CH-CM or PL-CM. CCA cells treated with DMEM+10% FBS served as controls. After allowing the cells to invade for 16 h, the cells that remained in the upper chamber and the upper membrane of the inserts were gently removed with a cotton swab. The cells that invaded the Matrigel and passed through the other side of the membrane were fixed with 3.7% formaldehyde, stained with 0.5% crystal violet and counted under a light microscope. The data are presented as the percentage of cell invasion compared with that of the untreated control (0% MSC-CM).

### Immunocytochemistry

To study the effect of MSC-CM on mesenchymal marker expression, the vimentin level in CCA cells was determined by immunofluorescence staining. KKU100  $(2.5 \times 10^5 \text{ cells/cm}^2)$ , KKU213A  $(1 \times 10^5 \text{ cells/cm}^2)$  and KKU213B  $(2.5 \times 10^5 \text{ cells/cm}^2)$  cells were seeded in 24-well plates and treated with 50% and 75% CH-CM or PL-CM for 16 h. CCA cells treated with DMEM+10% FBS served as controls. After treatment, the cells were permeabilized with 0.5% Triton X-100 for 5 min, fixed with 3.7% formaldehyde for 15 min, blocked with 5% FBS for 1 h at room temperature, washed twice with PBS and labeled with 1:250 Alexa Fluor\* 488 antibody overnight at 4 °C. The nuclei were visualized by staining with 1:1000 Hoechst 33342 for 15 min at room temperature. The fluorescence intensity ratio of vimentin/Hoechst 33342 was then determined using a fluorescence microplate reader

### Quantitative reverse transcription PCR (RT-qPCR)

RT-qPCR was used to investigate the effects of MSC-CM on the gene expression of CCA cells. After treating CCA cells with 75% CH-CM or 75% PL-CM for 16 h, total RNA was extracted using TRIzol reagent (Invitrogen, USA). The quality and concentration of RNA were determined via a spectrophotometer. The RNA samples were then reverse transcribed to cDNA using the Iscript<sup>™</sup> reverse transcription supermix (Bio-Rad, USA). Real-time PCR was performed using the SYBR Green PCR Kit (Bio-Rad, USA) on an Applied Biosystems StepOne Plus real-time PCR system using the following protocol: 40 cycles of denaturation at 95 °C for 15 s and annealing/amplification at 60 °C for 1 min. The level of glyceraldehyde-3-phosphate dehydrogenase (GAPDH) mRNA was used to calculate the relative quantification of the target gene in each sample using the  $2^{-\Delta\Delta Ct}$  method. CCA cells treated with DMEM+10% FBS served as controls. The list of primers used for RT-qPCR is shown in Table 1.

### Western immunoblot analysis

After treatment with 50% or 75% CH-CM or PL-CM for 16 h, the CCA cells were lysed with RIPA lysis solution (Cell Signaling, USA) containing a cocktail of protease inhibitors (Abcam, UK). From each lysate, a 20 µg protein sample was separated by 12% sodium dodecyl sulfate-polyacrylamide gel electrophoresis (SDS-PAGE), electrotransferred to nitrocellulose membranes, blocked with 5% skim milk at room temperature for 1 h and incubated at 4 °C overnight with primary antibodies against phosphoinositide 3-kinases (PI3K), phospho-PI3

Target gene	Forward primer (5'-3')	Reverse primer (5'-3')
AKT	CAAGTCCTTGCTTTCAGGGC	ATACCTGGTGTCAGTCTCCGA
PI3K	CAATCGGTGACTGTGTGGGA	ACAGGTCAATGGCTGCATCA
NFKB1	TGCAGCAGACCAAGGAGATG	CCAGTCACACATCCAGCTGT
NFKB2	TGCACTGCTTCAGAGTGGAG	GGCTAGATGCAAGGCTGTTC
MMP-2	ACCCAGATGTGGCCAACTAC	GAGTCCGTCCTTACCGTCAA
CCND1	CGTGGCCTCTAAGATGAAGG	CTGGCATTTTGGAGAGGAAG
MYC	TTTCGGGTAGTGGAAAACCA	CAGCAGCTCGAATTTCTTCC
ZEB1	TGTTGCTGATGTGGCTTTATG	GTCTGTTGGCAGGTCATCCT
ZEB2	GTACCTTCAGCGCAGTGACA	TTCTTCTCGTGGCGGTACTT
GAPDH	CGAGATCCCTCCAAAATCAA	TTCACACCCATGACGAACAT

**Table 1**. List of primers used for quantitative real-time RT-PCR.

kinase p85 (Tyr458)/p55 (Tyr199) (p-PI3K), protein kinase B (Akt), phospho-AKT Ser473 (p-AKT), E-cadherin, N-cadherin and matrix metalloproteinases-2 (MMP-2) (all from Cell Signaling, USA). The membrane was subsequently incubated with horseradish peroxidase (HRP)-conjugated mouse anti-rabbit or goat anti-mouse IgG (Jackson ImmunoResearch Laboratories, USA; 1:10,000 dilution) for 1 h at room temperature. Finally, the signals were detected with an enhanced chemiluminescence (ECL) system (Bio-Rad Laboratories, Inc.), and the level of  $\beta$ -actin was used to calculate the relative quantification of the target proteins in each sample. CCA cells treated with DMEM+10% FBS served as controls.

### Evaluation of PI3K/AKT signaling

Lysates from CCA cells cultured with 0% MSC-CM, 75% MSC-CM,  $20~\mu$ M LY294002 or a combination of 75% MSC-CM and  $20~\mu$ M LY294002 were harvested after 16 h of treatment. The protein levels of PI3K, p-PI3K, AKT and p-AKT were determined by Western blotting. Wound healing and Transwell invasion assays were also carried out as previously described to determine whether CH-CM and PL-CM inhibit CCA cell migration and invasion by inhibiting PI3K/AKT signaling.

### Statistical analysis

GraphPad Prism software version 8.0.2 was used to perform the statistical analysis. All data are presented as the means  $\pm$  standard errors of the means (SEMs) of at least 3 independent experiments for each group. One-way or two-way analysis of variance was used together with the Tukey post hoc test to analyze statistically significant differences between multiple groups. A P value less than 0.05 was considered statistically significant.

### Data availability

All data generated or analysed during this study are included in this published article and its supplementary information files.

Received: 17 March 2025; Accepted: 19 August 2025

Published online: 26 August 2025

### References

- 1. Kendall, T. et al. Anatomical, histomorphological and molecular classification of cholangiocarcinoma. Liver Int. 39, 7-18 (2019).
- 2. Florio, A. A. et al. Global trends in intrahepatic and extrahepatic cholangiocarcinoma incidence from 1993 to 2012. *Cancer.* 126, 2666–2678 (2020).
- Bertuccio, P. et al. Global trends in mortality from intrahepatic and extrahepatic cholangiocarcinoma. J. Hepatol. 71, 104–114 (2019).
- Gad, M. M. et al. Epidemiology of cholangiocarcinoma; united States incidence and mortality trends. Clin. Res. Hepatol. Gastroenterol. 44, 885–893 (2020).
- 5. Doherty, B., Nambudiri, V. E. & Palmer, W. C. Update on the diagnosis and treatment of cholangiocarcinoma. *Curr. Gastroenterol. Rep.* 19, 1–8 (2017).
- 6. Moris, D. et al. Advances in the treatment of intrahepatic cholangiocarcinoma: an overview of the current and future therapeutic landscape for clinicians. *CA Cancer J. Clin.* **73**, 198–222 (2023).
- 7. Banales, J. M. et al. Cholangiocarcinoma 2020: the next horizon in mechanisms and management. *Nat. Rev. Gastroenterol. Hepatol.* 17, 557–588 (2020).
- 8. Blechacz, B. Cholangiocarcinoma: current knowledge and new developments. Gut Liver. 11, 13 (2017).
- 9. Liang, Z. et al. Targeting the PI3K/AKT/mTOR pathway offer a promising therapeutic strategy for cholangiocarcinoma patients with high doublecortin-like kinase 1 expression. *J. Cancer Res. Clin. Oncol.* **150**, 342 (2024).
- 10. Jiang, N. et al. Role of PI3K/AKT pathway in cancer: the framework of malignant behavior. Mol. Biol. Rep. 47, 4587-4629 (2020).
- 11. Yothaisong, S. et al. Increased activation of PI3K/AKT signaling pathway is associated with cholangicarcinoma metastasis and PI3K/mTOR Inhibition presents a possible therapeutic strategy. *Tumor Biol.* 34, 3637–3648 (2013).
- 12. Berebichez-Fridman, R. & Montero-Olvera, P. R. Sources and clinical applications of mesenchymal stem cells: State-of-the-art review. Sultan Qaboos Univ. Med. J. 18, e264–e277 (2018).
- 13. Lan, T., Luo, M. & Wei, X. Mesenchymal stem/stromal cells in cancer therapy. J. Hematol. Oncol. 14, 1-16 (2021).
- 14. Timaner, M., Tsai, K. K. & Shaked, Y. The multifaceted role of mesenchymal stem cells in cancer. Semin. Cancer Biol. 60, 225–237 (2020).

- Wu, T. et al. Inhibitory role of bone marrow mesenchymal stem cells-derived exosome in non-small-cell lung cancer: microRNA-30b-5p, EZH2 and PI3K/AKT pathway. J. Cell. Mol. Med. 27, 3526–3538 (2023).
- Wang, Y., Lin, C. & Exosomes miR-22-3p derived from mesenchymal stem cells suppress colorectal cancer cell proliferation and invasion by regulating RAP2B and PI3K/AKT pathway. J. Oncol. 2021, 3874478 (2021).
- 17. Wu, S. et al. Human adipose–derived mesenchymal stem cells promote breast cancer MCF7 cell epithelial–mesenchymal transition by cross interacting with the TGF–β/Smad and PI3K/AKT signaling pathways. *Mol. Med. Rep.* **19**, 177–186 (2019).
- 18. Khan, W. S. & Hardingham, T. E. Mesenchymal stem cells, sources of cells and differentiation potential. J. Stem Cells. 7, 75 (2012).
- 19. Bieback, K. & Brinkmann, I. Mesenchymal stromal cells from human perinatal tissues: from biology to cell therapy. World J. Stem Cells. 2, 81–92 (2010).
- 20. Buettner, S. et al. Performance of prognostic scores and staging systems in predicting long-term survival outcomes after surgery for intrahepatic cholangiocarcinoma. *J. Surg. Oncol.* **116**, 1085–1095 (2017).
- 21. Yagi, H. & Kitagawa, Y. The role of mesenchymal stem cells in cancer development. Front. Genet. 4, 261 (2013).
- 22. Deans, R. J. & Moseley, A. B. Mesenchymal stem cells: biology and potential clinical uses. Exp. Hematol. 28, 875-884 (2000).
- 23. Akiyama, K. et al. Characterization of bone marrow derived mesenchymal stem cells in suspension. Stem Cell. Res. Ther. 3, 1–13 (2012).
- 24. Oedayrajsingh-Varma, M. et al. Adipose tissue-derived mesenchymal stem cell yield and growth characteristics are affected by the tissue-harvesting procedure. *Cytotherapy* **8**, 166–177 (2006).
- 25. Dabiri, S., Derakhshani, A., Vahidi, R. & Farsinejad, A. Peripheral blood-derived mesenchymal stem cells: growth factor-free isolation, molecular characterization and differentiation. *Iran. J. Pathol.* 13, 461–466 (2018).
- 26. Araújo, A. B. et al. Comparison of human mesenchymal stromal cells from four neonatal tissues: amniotic membrane, chorionic membrane, placental decidua and umbilical cord. *Cytotherapy* 19, 577–585 (2017).
- Chu, D. T. et al. An update on the progress of isolation, culture, storage, and clinical application of human bone marrow mesenchymal stem/stromal cells. Int. J. Mol. Sci. 21, 708 (2020).
- 28. Aithal, A. P., Bairy, L. K. & Seetharam, R. N. Safety and therapeutic potential of human bone marrow-derived mesenchymal stromal cells in regenerative medicine. Stem Cell. Investig. 8 (2021).
- 29. Stenderup, K., Justesen, J., Clausen, C. & Kassem, M. Aging is associated with decreased maximal life span and accelerated senescence of bone marrow stromal cells. *Bone*. 33, 919–926 (2003).
- 30. Baker, N., Boyette, L. B. & Tuan, R. S. Characterization of bone marrow-derived mesenchymal stem cells in aging. *Bone.* **70**, 37–47 (2015)
- 31. Vellasamy, S., Sandrasaigaran, P., Vidyadaran, S., George, E. & Ramasamy, R. Isolation and characterisation of mesenchymal stem cells derived from human placenta tissue. World J. Stem Cells. 4, 53–61 (2012).
- 32. Hass, R., Kasper, C., Böhm, S. & Jacobs, R. Different populations and sources of human mesenchymal stem cells (MSC): a comparison of adult and neonatal tissue-derived MSC. Cell. Commun. Signal. 9, 1–14 (2011).
- 33. Sagaradze, G. et al. Conditioned medium from human mesenchymal stromal cells: towards the clinical translation. *Int. J. Mol. Sci.* **20**, 1656 (2019).
- 34. Slama, Y. et al. The dual role of mesenchymal stem cells in cancer pathophysiology: pro-tumorigenic effects versus therapeutic potential. *Int. J. Mol. Sci.* 24, 13511 (2023).
- 35. Gunawardena, T. N. A., Rahman, M. T. & Abdullah, B. J. J. Abu kasim, N. H. Conditioned media derived from mesenchymal stem cell cultures: the next generation for regenerative medicine. *J. Tissue Eng. Regen. Med.* 13, 569–586 (2019).
- 36. Li, P. et al. Mesenchymal stem cell-conditioned medium promotes MDA-MB-231 cell migration and inhibits A549 cell migration by regulating insulin receptor and human epidermal growth factor receptor 3 phosphorylation. *Oncol. Lett.* 13, 1581–1586 (2017).
- 37. Folcuti, R. M. et al. The effect of human mesenchymal stem cells-conditioned media on glioblastoma cells viability in vitro. *Curr. Health Sci. J.* 41, 339–344 (2015).
- 38. Lee, J. H., Park, C. H., Chun, K. H. & Hong, S. S. Effect of adipose-derived stem cell-conditioned medium on the proliferation and migration of B16 melanoma cells. *Oncol. Lett.* 10, 730–736 (2015).
- 39. Jantalika, T. et al. Human chorion-derived mesenchymal stem cells suppress JAK2/STAT3 signaling and induce apoptosis of cholangiocarcinoma cell lines. Sci. Rep. 12, 11341 (2022).
- 40. Jantalika, T. et al. The human placental amniotic membrane mesenchymal-stromal-cell-derived conditioned medium inhibits growth and promotes apoptosis of human cholangiocarcinoma cells in vitro and in vivo by suppressing IL-6/JAK2/STAT3 signaling. Cells. 12, 2788 (2023).
- 41. Yuan, Y. et al. Suppression of tumor cell proliferation and migration by human umbilical cord mesenchymal stem cells: A possible role for apoptosis and Wnt signaling. Oncol. Lett. 15, 8536–8544 (2018).
- 42. Liu, C. et al. Bone marrow mesenchymal stem cells promote head and neck cancer progression through Periostin-mediated phosphoinositide 3-kinase/Akt/mammalian target of Rapamycin. Cancer Sci. 109, 688–698 (2018).
- 43. De Boeck, A. et al. Bone marrow-derived mesenchymal stem cells promote colorectal cancer progression through paracrine neuregulin 1/HER3 signalling. *Gut* 62, 550–560 (2013).
- 44. Ryu, H. S. et al. Overexpression of epithelial-mesenchymal transition-related markers according to cell dedifferentiation: clinical implications as an independent predictor of poor prognosis in cholangiocarcinoma. *Hum. Pathol.* 43, 2360–2370 (2012).
- 45. Aiello, N. M. & Kang, Y. Context-dependent EMT programs in cancer metastasis. J. Exp. Med. 216, 1016–1026 (2019).
- Savagner, P., Gilles, C., Newgreen, D. F., Sato, H. & Thompson, E. W. Springer, Matrix metalloproteases and epithelial-tomesenchymal transition: implications for carcinoma metastasis. Rise and fall of epithelial phenotype: concepts of epithelialmesenchymal transition (ed. Savagner, P.) 297–315 (2005).
- 47. Ghafouri-Fard, S. et al. Role of PI3K/AKT pathway in squamous cell carcinoma with an especial focus on head and neck cancers. *Cancer Cell. Int.* 22, 1–27 (2022).
- 48. Sarris, E. G., Saif, M. W. & Syrigos, K. N. The biological role of PI3K pathway in lung cancer. Pharmaceuticals 5, 1236–1264 (2012).
- 49. Paskeh, M. D. A. et al. Biological impact and therapeutic perspective of targeting PI3K/Akt signaling in hepatocellular carcinoma: promises and challenges. *Pharmacol. Res.* **187**, 106553 (2023).
- 50. Corti, F. et al. Targeting the PI3K/AKT/mTOR pathway in biliary tract cancers: A review of current evidences and future perspectives. Cancer Treat. Rev. 72, 45–55 (2019).
- Lu, L. et al. Bone marrow mesenchymal stem cells suppress growth and promote the apoptosis of glioma U251 cells through downregulation of the PI3K/AKT signaling pathway. Biomed. Pharmacother. 112, 108625 (2019).
- 52. Liu, J., Han, G., Liu, H. & Qin, C. Suppression of cholangiocarcinoma cell growth by human umbilical cord mesenchymal stem cells: a possible role of Wnt and Akt signaling. *PLoS One.* 8, e62844 (2013).
- 53. Wang, M. et al. Inhibition of STAT3 signaling as critical molecular event in HUC-MSCs suppressed glioblastoma cells. *J. Cancer.* 14, 611–627 (2023).
- 54. Li, M. et al. Perichondrium mesenchymal stem cells inhibit the growth of breast cancer cells via the DKK-1/Wnt/β-catenin signaling pathway. *Oncol. Rep.* **36**, 936–944 (2016).
- 55. Dokduang, H. et al. Survey of activated kinase proteins reveals potential targets for cholangiocarcinoma treatment. *Tumor Biol.* **34**, 3519–3528 (2013).
- Idris, R., Chaijaroenkul, W. & Na-Bangchang, K. Molecular targets and signaling pathways in cholangiocarcinoma: A systematic review. Asian Pac. J. Cancer Prev. 24, 741–751 (2023).

- 57. Yulyana, Y. et al. Paracrine factors of human fetal MSCs inhibit liver cancer growth through reduced activation of IGF-1R/PI3K/Akt signaling. *Mol. Ther.* 23, 746–756 (2015).
- 58. Wang, Y. & Lin, C. Exosomes miR-22-3p derived from mesenchymal stem cells suppress colorectal cancer cell proliferation and invasion by regulating RAP2B and PI3K/AKT pathway. *J. Oncol.* **2021**, 3874478 (2021).
- Li, T. et al. Mesenchymal stem cell-derived exosomal microRNA-3940-5p inhibits colorectal cancer metastasis by targeting integrin α6. Dig. Dis. Sci. 66, 1916–1927 (2021).
- 60. Xu, Z. et al. Mesenchymal stem cell-derived exosomes carrying microRNA-150 suppresses the proliferation and migration of osteosarcoma cells via targeting IGF2BP1. Transl. Cancer Res. 9, 5323–5335 (2020).
- 61. Xu, H. et al. Mesenchymal stem cell-derived exosomal microRNA-133b suppresses glioma progression via Wnt/β-catenin signaling pathway by targeting EZH2. Stem Cell. Res. Ther. 10, 381 (2019).
- 62. Jung, P. Y. et al. Adipose tissue-derived mesenchymal stem cells cultured at high density express IFN-β and TRAIL and suppress the growth of H460 human lung cancer cells. *Cancer Lett.* **440**, 202–210 (2019).
- 63. Byun, C. S. et al. Adipose tissue-derived mesenchymal stem cells suppress growth of Huh7 hepatocellular carcinoma cells via interferon (IFN)-β-mediated JAK/STAT1 pathway in vitro. *Int. J. Med. Sci.* 17, 609–619 (2020).
- 64. Clarke, M. R., Imhoff, F. M. & Baird, S. K. Mesenchymal stem cells inhibit breast cancer cell migration and invasion through secretion of tissue inhibitor of metalloproteinase-1 and-2. *Mol. Carcinog.* 54, 1214–1219 (2015).
- 65. Sripa, B. et al. Establishment and characterization of an opisthorchiasis-associated cholangiocarcinoma cell line (KKU-100). World J. Gastroenterol. 11, 3392–3397 (2005).
- Sripa, B. et al. Functional and genetic characterization of three cell lines derived from a single tumor of an Opisthorchis viverriniassociated cholangiocarcinoma patient. Hum. Cell. 33, 695–708 (2020).
- 67. Dominici, M. et al. Minimal criteria for defining multipotent mesenchymal stromal cells. The international society for cellular therapy position statement. *Cytotherapy*. **8**, 315–317 (2006).

### **Acknowledgements**

The authors thank the delivery room staff at Thammasat University Hospital for facilitating the collection of the samples. This research was supported by Thailand Science Research and Innovation (TSRI) Fundamental Fund, fiscal year 2024 (contract no. TUFF 55/2567), Thammasat University and Center of Excellence in Stem Cell Research, Thammasat University (to C. Tantrawatpan). This study was supported by Thammasat Postdoctoral Fellowship (to T. Jantalika).

### **Author contributions**

S.M., P.K., L.P., and C.T.: conceptualization; T.J., S.M., and C.T.: data curation; T.J., S.M., D.T., and C.T.: formal analysis; all authors: validation and methodology, S.P., and C.T.: resources; P.K., L.P., and C.T.: supervision; C.T.: project administration; T.J., P.K., L.P., and C.T.: writing-original draft; P.K., L.P., and C.T.: writing-review and editing. All authors read and agreed the submitted version of the manuscript.

### **Declarations**

### Competing interests

The authors declare no competing interests.

### Additional information

**Supplementary Information** The online version contains supplementary material available at https://doi.org/1 0.1038/s41598-025-16789-6.

**Correspondence** and requests for materials should be addressed to L.P. or C.T.

Reprints and permissions information is available at www.nature.com/reprints.

**Publisher's note** Springer Nature remains neutral with regard to jurisdictional claims in published maps and institutional affiliations.

**Open Access** This article is licensed under a Creative Commons Attribution-NonCommercial-NoDerivatives 4.0 International License, which permits any non-commercial use, sharing, distribution and reproduction in any medium or format, as long as you give appropriate credit to the original author(s) and the source, provide a link to the Creative Commons licence, and indicate if you modified the licensed material. You do not have permission under this licence to share adapted material derived from this article or parts of it. The images or other third party material in this article are included in the article's Creative Commons licence, unless indicated otherwise in a credit line to the material. If material is not included in the article's Creative Commons licence and your intended use is not permitted by statutory regulation or exceeds the permitted use, you will need to obtain permission directly from the copyright holder. To view a copy of this licence, visit <a href="https://creativecommons.org/licenses/by-nc-nd/4.0/">https://creativecommons.org/licenses/by-nc-nd/4.0/</a>.

© The Author(s) 2025